Journal of System Simulation

Volume 30 | Issue 12 Article 34

1-3-2019

# Key Points Analysis and Simulation for System Design of Airborne WAS-GMTI Radar

Yan He
*College of Information Science and Technology, Nanjing University of Aeronautics and Astronautics, Nanjing 210016, China;*

Daiyin Zhu
*College of Information Science and Technology, Nanjing University of Aeronautics and Astronautics, Nanjing 210016, China;*

# Key Points Analysis and Simulation for System Design of Airborne WAS-GMTI Radar


## Abstract

Abstract: Wide area surveillance-ground moving target detection (WAS-GMTI) mode is one of the important modes for most multi-functional airborne radar. System design of the WAS-GMTI mode can affect the final moving targets detection and tracking abilities to a great extent. Therefore, research focuses on the system design of multi-channel WAS-GMTI radar system. *The expression of WAS-GMTI radar echo (including the crab angle) is derived. Signal to noise ratio (SNR) and clutter to noise ratio (CNR) are presented. These are the preparations and foundations for the further discussion. Four key points are detailedly analyzed in the process of system design of WAS-GMTI radar, including range walk and range curvature analysis, clutter spectrum analysis, multi-frequency system and multi-PRF system analysis, number of pulses per burst analysis. Besides, these four key points are simulated and some conclusions are drawn after each discussion.*



## Keywords

wide-area surveillance, ground moving target indication, radar echo, system design

## Recommended Citation

Yan He, Zhu Daiyin. Key Points Analysis and Simulation for System Design of Airborne WAS-GMTI Radar[J]. Journal of System Simulation, 2018, 30(12): 4760-4769.

第 30 卷第 12 期 系统仿真学报© Vol. 30 No. 12
2018 年 12 月 Journal of System Simulation Dec., 2018

# Key Points Analysis and Simulation for System Design of Airborne WAS-GMTI Radar

*Yan He, Zhu Daiyin*

(College of Information Science and Technology, Nanjing University of Aeronautics and Astronautics, Nanjing 210016, China)

**Abstract:** Wide area surveillance-ground moving target detection (WAS-GMTI) mode is one of the important modes for most multi-functional airborne radar. System design of the WAS-GMTI mode can affect the final moving targets detection and tracking abilities to a great extent. Therefore, research focuses on the system design of multi-channel WAS-GMTI radar system. *The expression of WAS-GMTI radar echo (including the crab angle) is derived. Signal to noise ratio (SNR) and clutter to noise ratio (CNR) are presented. These are the preparations and foundations for the further discussion. Four key points are detailedly analyzed in the process of system design of WAS-GMTI radar, including range walk and range curvature analysis, clutter spectrum analysis, multi-frequency system and multi-PRF system analysis, number of pulses per burst analysis. Besides, these four key points are simulated and some conclusions are drawn after each discussion.*

**Keywords:** wide-area surveillance; ground moving target indication; radar echo; system design

# 机载广域监视雷达系统设计要点分析与仿真

闫贺，朱岱寅

(南京航空航天大学电子信息工程学院，南京 210016)

**摘要:** 机载广域监视模式是多功能机载雷达的重要模式之一。对广域监视模式进行的系统设计将在很大程度上影响最终动目标的检测及跟踪效果。因此，我们重点研究了多通道广域监视雷达的系统设计问题。*推导了含有偏流角信息的广域监视雷达回波表达式。给出了系统信噪比和杂噪比的计算方法。这些都是进行系统设计的基础。详细分析了广域监视雷达系统设计时的四个关键因素，包括：距离走动和距离弯曲分析，杂波谱分析，多载频系统和多 PRF 系统分析，每个波位脉冲数分析。这四个关键因素都进行了仿真并在仿真后给出了相关结论。*

**关键词:** 广域监视；地面运动目标指示；雷达回波；系统设计

中图分类号：TP391.9 文献标识码：A 文章编号：1004-731X (2018) 12-4760-10

DOI: 10.16182/j.issn1004731x.joss.201812034

## Introduction

WAS-GMTI mode occupies an important place in most airborne surveillance radar[1-8]. This mode is realized by antenna scanning in the azimuth direction periodically. Therefore, the same section of the ground is scanned successively and a wide area can be monitored. Besides, the same moving object can be illuminated from different aspect angle via the scan operation, which improves the target detection ability and permits a meaningful target tracking [1].

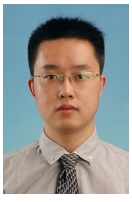

Received: 2016-08-26 Revised: 2017-01-05;
Foundation item: General Program of National Natural Science Foundation of China (61501231), Jiangsu Provincial Natural Science Foundation (BK20150759), Aeronautical Science Foundation of China (20152052027)
Biography: Yan He (1985-), male, Jiangsu, China, Ph.D. degree, research interests: air-borne/space-borne synthetic aperture radar (SAR) system design and multichannel SAR signal processing.

It is known that appropriate system parameters and signal processing algorithm can make the radar system reach its perfect performance. However, recent researches mainly focus on the signal processing algorithm of the WAS-GMTI mode and seldom refer to the WAS-GMTI system design[1, 7-12]. Only in the front section of paper[1], which introduces the WAS-GMTI mode of PAMIR (Phased Array Multifunctional Imaging Radar) system, the following three points about WAS-GMTI system design are discussed.

1. The antenna beam width should be carefully chosen to find a compromise between the target positioning accuracy and target revisit time.

2. The theoretical expression for the illuminated area and azimuth scan angle is derived.

3. The number of look directions should be chosen to guarantee at least a half overlap of the footprints of two subsequent azimuth look directions.

In this paper, we make a further investigation on the WAS-GMTI system design. Firstly, the radar echo formula (including ground clutter and moving targets) of WAS-GMTI mode is derived. The formula is more close to the real condition since the crab angle is considered in the derivation. Secondly, the expression of SNR and CNR are presented in the process of signal processing. The aforementioned derivations are the foundations for the further discussion. Then, four key points are investigated, which can be regarded as the supplements for the discussion in Ref. [1]. These points include the expression for range walk and range curvature, the expression for clutter spectrum, selection of multi-frequency system and multi-PRF system, selection of number of pulses per burst. Besides, some conclusions are drawn after each discussion. The study shows that all these points should be carefully considered before the real WAS-GMTI system design.

## 1 Radar echo formula derivation

The 3-D geometry of an airborne WAS-GMTI radar system is shown in Fig. 1. There are $M$ receive channels placed along the y-direction, and the radar signal is transmitted from the first channel. The distance between the $m$ th channel and the first channel is represented as $L_m$. Hence, $L_1$=0. Assume the platform flights with a crab angle $\theta_{crab}$ away from the y-direction, and its flight velocity and altitude are denoted as $V_p$ and $H$ respectively. In the scene, a moving target moves with a ground velocity $V_t$ toward the platform. The x-component and y-component velocity of the moving target is represented as $V_{tx}$ and $V_{ty}$ respectively, and the angle between $V_t$ and $V_{ty}$ is denoted as $\phi_t$. Besides, the azimuth angle and elevation angle of the targets are $\theta_t$ and $\varphi_t$ relative to the platform, and the starting distance between the target and the platform is $R_t$.

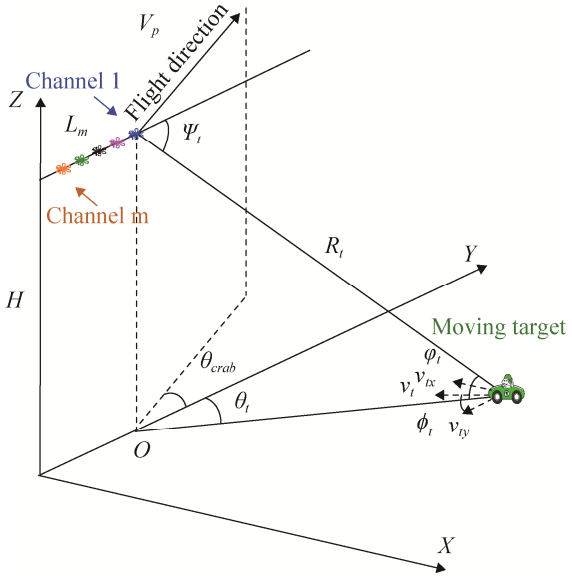


Fig. 1 3-D geometry of WAS-GMTI radar

Then, the received echo of the $m$ th channel can be expressed by[7-9, 13-15]

$$S_{\mathrm{m}}(\tau,\eta)=\sqrt{P_m}\cdot\mathrm{rect}\left(\frac{\eta}{K\cdot T_a}\right)\times \mathrm{rect}\left(\frac{\tau-\frac{R_{\mathrm{l}\_t}(\eta)+R_{\mathrm{m}\_t}(\eta)}{c}}{T_r}\right)\times \exp\left\{-j\times 2\pi\times\frac{R_{\mathrm{l}\_t}(\eta)+R_{\mathrm{m}\_t}(\eta)}{\lambda}\right\} \exp\left\{j\times\pi\times K_r\times\left(\tau-\frac{R_{\mathrm{l}\_t}(\eta)+R_{\mathrm{m}\_t}(\eta)}{c}\right)^2\right\} \quad (1)$$

Where: $m$ Index of onboard channels, $m=1,2,\ldots,M$ ($M$ is the number of channels); $\tau$ Range time; $\eta$ Azimuth time; $P_m$ Received power of the $m$ th channel; $K$ Number of pulses in one burst; $T_a$ Pulse repetition time; $R_{m\_t}(\eta)$ Range between the $m$ th channel and the target, $m=1,2,\ldots,M$ ; $c$ Propagating velocity of light; $T_r$ Duration of the transmitted pulse; $\lambda$ Radar operating wavelength; $K_r$ Range frequency modulation rate; $j$ Complex constant, $\sqrt{-1}$ .

According to the geometry of the WAS-GMTI system shown in Fig. 1, the square form of $R_{\mathrm{l}\_t}(\eta)$ can be written as

$$\begin{aligned}R_{\mathrm{l}\_t}^2(\eta)=&(R_t\times\cos(\varphi_t)\times\cos(\theta_t)-V_p\times\\&\eta\times\cos(\theta_{\mathrm{crab}})-V_t\times\eta\times\cos(\phi_t))^2+\\&H^2+(R_t\times\cos(\varphi_t)\times\sin(\theta_t)+\\&V_p\times\eta\times\sin(\theta_{\mathrm{crab}})-V_t\times\eta\times\sin(\phi_t))^2=\\&R_t^2\times\cos^2(\varphi_t)+H^2+\\&(V_p^2+V_t^2+2\times V_p\times V_t\times\cos(\theta_{\mathrm{crab}}+\phi_t))\times\\&\eta^2-2\times R_t\times\cos(\varphi_t)\times\\&(V_p\times\cos(\theta_t+\theta_{\mathrm{crab}})+V_t\times\cos(\theta_t-\phi_t))\times\eta\end{aligned} \quad (2)$$

Thus, $R_{m\_t}(\eta)$ can be approximated by

$$R_{m\_t}(\eta)\cong R_{\mathrm{l}\_t}(\eta)+L_m\cdot\cos(\theta_t)\cdot\cos(\varphi_t) \quad (3)$$

Equation (1) presents the radar echo formula of a moving target. If let $V_t=0$, we can obtain the radar echo formula of the stationary ground clutter.

After range compression, the radar echo can be given by (neglect range straddling losses)

$$Z_{\mathrm{m}}(\tau,\eta)=\sqrt{P_m}\times(K_r\times T_r^2)\times\mathrm{rect}\left(\frac{\eta}{K\cdot T_a}\right)\times \exp\left\{-j\times 2\pi\times\frac{R_{\mathrm{l}\_t}(\eta)+R_{\mathrm{m}\_t}(\eta)}{\lambda}\right\}\times \sin\mathrm{c}\left\{K_r\times T_r\times\left(\tau-\frac{R_{\mathrm{l}\_t}(\eta)+R_{\mathrm{m}\_t}(\eta)}{c}\right)\right\} \quad (4)$$

where $K_r\cdot T_r^2$ represents the coherent integration of the target in the process of range compression. Compared with the SAR imaging mode, the WAS-GMTI mode is often designed with lower range resolution, and therefore the following approximation is reasonable.

$$\sin\mathrm{c}\left\{K_rT_a\left(\tau-\frac{R_{\mathrm{l}\_t}(\eta)+R_{\mathrm{m}\_t}(\eta)}{c}\right)\right\}\simeq \sin\mathrm{c}\left\{K_rT_a\left(\tau-\frac{2\cdot R_{\mathrm{l}\_t}(\eta)}{c}\right)\right\} \quad (5)$$

Then, azimuth weighted FFT (Fast Fourier Transform) is performed to transform the data to the range-Doppler domain for further processing such as clutter suppression, CFAR detection and parameter estimation. If we neglect range walk and Doppler straddling losses herein, the echo formula can be further expressed by

$$E_{\mathrm{m}}(\tau,f_\eta)=\sqrt{P_m}\times(K_r\times T_r^2)\times\left(\sum_{k=1}^{K}w_k\right)\times \sin\mathrm{c}\left\{K_r\times T_r\times\left(\tau-2\times\frac{R_{\mathrm{l}\_t}(\eta)}{c}\right)\right\}\times w_a\left(K\times T_a\times\left(f_\eta-2\times\frac{\left(V_p\times\cos(\theta_t+\theta_{\mathrm{crab}})+V_t\times\cos(\theta_t-\phi_t)\right)\times\cos(\varphi_t)}{\lambda}\right)\right) \quad (6)$$

where $\boldsymbol{w_a}=[w_1,w_2,\ldots,w_K]^T$ denotes the weighting coefficient of azimuth weighted FFT. In Equation (6), $\sum_{k=1}^{K}w_k$ represents the coherent integration of the target in the process of azimuth weighted FFT.

## 2 SNR and CNR derivation

Based on the radar equation, $P_m$ can be given by

$$P_m = \frac{P_0 \cdot G_t(\theta_t,\varphi_t) \cdot G_r(\theta_t,\varphi_t) \cdot \lambda^2 \cdot \sigma_t}{(4\pi)^3 \cdot R_{m\_t}^4 \cdot L_s} \quad (7)$$

Where: $P_0$ Transmit power; $G_t(\theta_t,\varphi_t)$ Gain of the radar transmit antenna (relative to the target); $G_r(\theta_t,\varphi_t)$ Gain of the radar receive antenna (relative to the target); $\sigma_t$ Radar cross-section of the target; $L_s$ System losses.

The data of WAS-GMTI mode are processed per scan and per antenna look direction respectively [1-2], and the observation time allocated to one look direction is so short that the impact on the radar equation from the changes of $R_{m\_t}$ can be neglected in the same look direction. Besides, for the radar equation, the influence from channel intervals can also be neglected. Therefore, the received power of all the channels can be uniformly given by

$$P_t = \frac{P_0 \cdot G_t(\theta_t,\varphi_t) \cdot G_r(\theta_t,\varphi_t) \cdot \lambda^2 \cdot \sigma_t}{(4\pi)^3 \cdot R_t^4 \cdot L_s} \quad (8)$$

The thermal noise power can be written as

$$P_\sigma = k \cdot T_0 \cdot B_r \cdot F_n \quad (9)$$

Where: $k$ Boltzmann constant; $T_0$ Temperature; $B_r$ Receiver bandwidth; $F_n$ Noise Factor.

Then, the SNR on the receiver can be expressed by

$$SNR_t = \frac{P_t}{P_\sigma} = \frac{P_0 \cdot G_t(\theta_t,\varphi_t) \cdot G_r(\theta_t,\varphi_t) \cdot \lambda^2 \cdot \sigma_t}{(4\pi)^3 \cdot R_t^4 \cdot L_s \cdot k \cdot T_0 \cdot B_r \cdot F_n} \quad (10)$$

According to Equation (4), after range compression the power of the target can be calculated by

$$P_{t\_r} = \frac{P_0 \times G_t(\theta_t,\varphi_t) \times G_r(\theta_t,\varphi_t) \times \lambda^2 \times \sigma_t}{(4\pi)^3 \times R_t^4 \times L_s} \times (K_r \times T_r^2)^2 \quad (11)$$

Since the noise component is non-coherent integration in the process of range compression, the power of the noise component after range compression can be expressed as follows:

$$P_{\sigma\_r} = k \cdot T_0 \cdot B_r \cdot F_n \cdot (K_r \cdot T_r^2) \quad (12)$$

Therefore, the SNR after range compression is obtained from Equation (11) and (12)

$$SNR_{t\_r} = P_{t\_r} / P_{\sigma\_r} = \frac{P_0 \times G_t(\theta_t,\varphi_t) \times G_r(\theta_t,\varphi_t) \times \lambda^2 \times \sigma_t}{(4\pi)^3 \times R_t^4 \times L_s \times k \times T_0 \times B_r \times F_n} \times (K_r \times T_r^2) \quad (13)$$

After azimuth weighted FFT, the target power, the noise power and SNR can also be obtained, and they are given as follows:

$$P_{t\_ra} = \frac{P_0 \times G_t(\theta_t,\varphi_t) \times G_r(\theta_t,\varphi_t) \times \lambda^2 \times \sigma_t}{(4\pi)^3 \times R_t^4 \times L_s} \times (K_r \times T_r^2)^2 \times \left( \sum_{k=1}^{K} w_k \right)^2 \quad (14)$$

$$P_{\sigma\_ra} = k \cdot T_0 \cdot B_r \cdot F_n \cdot (K_r \cdot T_r^2) \cdot \left( \sum_{k=1}^{K} w_k^2 \right) \quad (15)$$

$$SNR_{t\_ra} = P_{t\_ra} / P_{\sigma\_ra} = \frac{P_0 \times G_t(\theta_t,\varphi_t) \times G_r(\theta_t,\varphi_t) \times \lambda^2 \times \sigma_t}{(4\pi)^3 \times R_t^4 \times L_s \times k \times T_0 \times B_r \times F_n} \times (K_r \times T_r^2) \times \left( \sum_{k=1}^{K} w_k \right)^2 \Big/ \left( \sum_{k=1}^{K} w_k^2 \right) \quad (16)$$

Aside from the calculation of radar cross-section, the changes of CNR in the process of signal processing can be obtained in the same way.

To calculate the CNR of one range-Doppler cell, the radar cross-section of that range-Doppler cell can be written as (see Fig. 2)

$$\sigma_c = \sigma_0 \cdot R_c \cdot \Delta\theta \cdot \frac{\Delta R}{\cos(\varphi_c)} \quad (17)$$

where $R_c$ denotes the distance of the range-Doppler cell, $\Delta R$ and $\Delta\theta$ represents the range resolution and azimuth angle resolution of that range-Doppler cell respectively, $\varphi_c$ is the elevation angle of the range-Doppler cell, $\sigma_0$ is the area reflectivity of the ground clutter at the location of the range-Doppler cell to be calculated.

Note that the azimuth angle resolution $\Delta\theta$ denotes the angular width relative to one Doppler cell



https://dc-china-simulation.researchcommons.org/journal/vol30/iss12/34
DOI: 10.16182/j.issn1004731x.joss.201812034

and it changes with the azimuth scan angle. It is known that the azimuth frequency resolution is $\frac{PRF}{K}$, where $PRF$ is pulse repetition frequency, and it can be written as

$$\frac{PRF}{K}=\left|\frac{2V_p}{\lambda}\times\cos\left(\theta_{\text{crab}}+\theta_c+\frac{\Delta\theta}{2}\right)\times\cos(\varphi_c)-\frac{2V_p}{\lambda}\times\cos\left(\theta_{\text{crab}}+\theta_c-\frac{\Delta\theta}{2}\right)\times\cos(\varphi_c)\right| \quad (18)$$

where $\theta_c$ is the azimuth angle corresponding to the Doppler cell.

Solving this equation yields

$$\Delta\theta=\frac{\lambda\cdot PRF}{2V_p\cdot K\cdot\cos(\varphi_c)\cdot\sin(\theta_{crab}+\theta_c)} \quad (19)$$

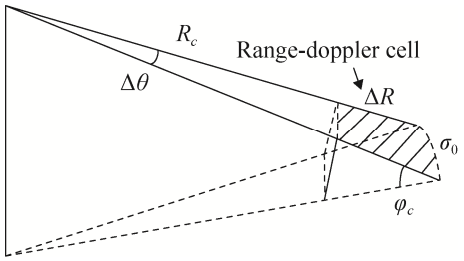


Fig. 2 Radar cross-section of one range-Doppler cell

According to Equation (13), (16), (17) and (19), the CNR of one range-Doppler cell in the process of signal processing can be calculated. Note that in the process of SNR and CNR calculation, range ambiguities and azimuth frequency ambiguities should also be taken into consideration, which are not discussed in detail herein.

## 3 Key points analysis in the system design of WAS-GMTI mode

Before the key points analysis, we want to discuss about the scan schemes of WAS-GMTI mode. There are two scan schemes for electronic scanning system which are shown in Fig. 3. In the first scheme, the antenna scans from A to B, then it jumps to A and repeats the operation (A→B, A→B, A→B,…). However, in the second scheme, after the antenna scans from A to B, it scans back to A from B, and then it repeats the operation (A→B, B→A, A→B,…). Theoretically, a moving target can be detected in several successive scan periods. The time interval between the same target detections is almost the same in the first scheme, but it varies in the second scheme, especially when the target is near A side or B side. It is known that the equal time interval between target detection is more beneficial for target tracking. Therefore, the first scan manner is preferred in the real WAS-GMTI system design.

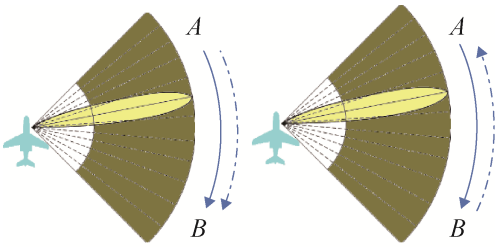


Fig. 3 Two scan schemes for WAS-GMTI system

Then we discuss about four key points in the system design of WAS-GMTI mode. In order to facilitate the later discussion, a set of typical parameters of the WAS-GMTI mode is presented in Tab. 1. Note that these parameters will be used in the following simulation experiment [1].

Tab. 1 Typical parameters of an airborne WAS-GMTI system

| | | | |
|---|---|---|---|
| Pulse repetition frequency | 3 kHz | Center frequency | 9.45 GHz |
| Platform velocity | 110 m/s | Altitude of the platform | 6.4 km |
| Azimuth scan angle | 40°~ 140° | Step angle | 2° |
| Channel spacing (uniformly distributed) | 0.32 m | Crab angle | 7.5° |
| Window function of azimuth FFT | 70 db Chebyshev window | Slant range | 75 km |

### 3.1 Range walk and range curvature analysis

To analyze the range walk in the WAS-GMTI mode, it is helpful to expand the range function $R_{l\_t}(\eta)$ in equation (2) as a Taylor series as follows:

$$R_{l\_t}(\eta)=R_{l\_t}(0)+R_{l\_t}'(0)\times\eta+\frac{1}{2}\times R_{l\_t}''(0)\cdot\eta^2+\cdots=R_t-(V_p\cdot\cos(\theta_t+\theta_{\text{crab}})+V_t\times\cos(\theta_t-\phi_t))\times\cos(\varphi_t)\times\eta+\frac{1}{2}\times\frac{(V_p^2+V_t^2+2\times V_p\times V_t\times\cos(\theta_{\text{crab}}+\phi_t))}{R_t}\times\eta^2+\cdots \quad (20)$$

In such an expansion, it is often possible to neglect terms of order higher than the quadratic, and the linear part of this is range walk and the quadratic part is range curvature. That is

$$P_{\text{range\_walk}}=(V_p\cdot\cos(\theta_t+\theta_{\text{crab}})+V_t\cdot\cos(\theta_t-\phi_t))\cdot\cos(\varphi_t)\cdot\eta \quad (21)$$

$$P_{\text{range\_curvature}}=\frac{1}{2}\times\frac{(V_p^2+V_t^2+2\times V_p\times V_t\times\cos(\theta_{\text{crab}}+\phi_t))}{R_t}\times\eta^2 \quad (22)$$

The maximal value of $P_{\text{range\_curvature}}$ with different $\theta_{\text{crab}}$ and $\phi_t$ is

$$P_{range\_curvature\_\max}=\frac{1}{2}\cdot\frac{(V_p+|V_t|)^2}{R_t}\cdot\eta^2 \quad (23)$$

According to the aforementioned parameters in Tab 1, we can obtain the maximal range curvature results with different target velocities $V_t$ and different integration time per look direction $\eta$.

From Fig. 4(a), it can be seen that range curvature is so small that it is negligible. In Equation (21), range walk comprises two components, one component is from the movement of the platform (it also denotes the range walk of clutter) and the other is from the movement of moving targets. That is

$$P_{\text{range\_walk\_platform}}=V_p\cdot\cos(\theta_t+\theta_{\text{crab}})\cdot\cos(\varphi_t)\cdot\eta \quad (24)$$

$$P_{\text{range\_walk\_target}}=V_t\cdot\cos(\theta_t-\phi_t)\cdot\cos(\varphi_t)\cdot\eta \quad (25)$$

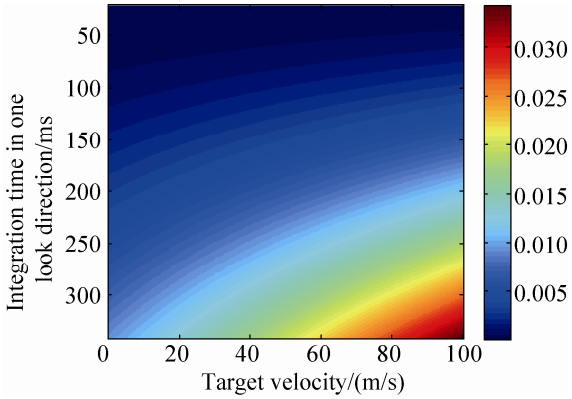


(a) Range curvature of WAS-GMTI mode in the typical airborne system parameters (unit: m)

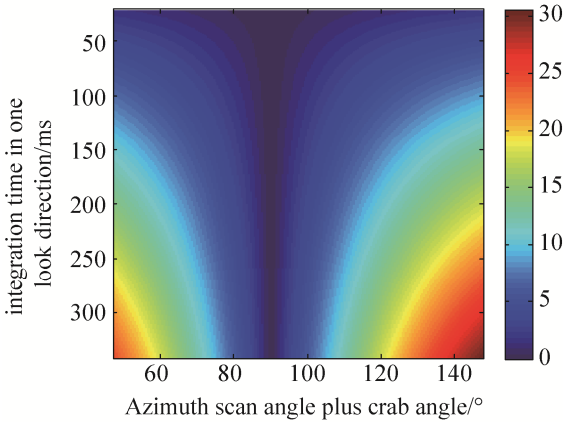


(b) Range walk from the movement of the platform (unit: m)

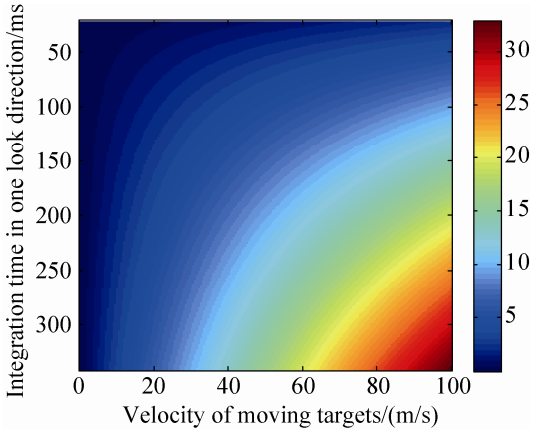


(c) Range walk from the movement of moving targets (unit: m)

Fig. 4 Range walk and range curvature analysis

It is easy to find that $V_t\cdot\cos(\theta_t-\phi_t)\cdot\cos(\varphi_t)\cdot\eta$ denotes the projection of the moving target on the radial direction (see Fig. 1), and it is maximal value is $V_t\cdot\cos(\varphi_t)\cdot\eta$. According to Tab. 1, $P_{\text{range\_walk\_platfrom}}$ and $P_{\text{range\_walk\_target}}$ can be calculated with



https://dc-china-simulation.researchcommons.org/journal/vol30/iss12/34
DOI: 10.16182/j.issn1004731x.joss.201812034

corresponding variables. The results are shown in Fig. 4(b) and Fig. 4(c) respectively.

Depending on different parameters, range walk of moving targets can make the power of the targets disperse in several neighboring range cells, which is unfavorable for moving targets detection. From Fig. 4(b) and Fig. 4(c), it can be seen that range walk increases with the integration time in one look direction.

**Conclusion**: To reduce the impact of range walk, the integration time in one look direction and the range of azimuth scan angle should be carefully designed according to the aforementioned derivation.

## 3.2 Clutter spectrum analysis

The azimuth frequency of clutter component can be expressed by

$$F_c = \frac{2V_p}{\lambda} \cdot \cos(\theta_{\text{crab}} + \theta_c) \cdot \cos(\varphi_c) \tag{26}$$

The width of clutter spectrum changes with different scan angles, and it can be written as

$$B_c(\theta_c) = \left| \frac{2V_p}{\lambda} \times \cos\left( \theta_{\text{crab}} + \theta_c + \frac{\theta_{3db}(\theta_c)}{2} \right) \times \cos(\varphi_c) - \frac{2V_p}{\lambda} \times \cos\left( \theta_{\text{crab}} + \theta_c - \frac{\theta_{3db}(\theta_c)}{2} \right) \times \cos(\varphi_c) \right| =$$

$$\frac{4V_p}{\lambda} \times \cos(\varphi_c) \times \sin(\theta_{\text{crab}} + \theta_c) \times \sin\left( \frac{\theta_{3db}(\theta_c)}{2} \right) =$$

$$\frac{2V_p}{\lambda} \times \cos(\varphi_c) \times \sin(\theta_{\text{crab}} + \theta_c) \times \theta_{3db}(\theta_c) \tag{27}$$

where $\theta_{3db}(\theta_c)$ denotes 3db antenna bandwidth, and it is a function of azimuth scan angle. According to the basic antenna theory, $\theta_{3db}(\theta_c)$ can be further expressed by

$$\theta_{3db}(\theta_c) = \frac{\theta_{3db\_0}}{\sin(\theta_c)} \tag{28}$$

where $\theta_{3db\_0}$ is the 3db antenna bandwidth in the side-looking condition.

Then, equation (27) can be further written as

$$B_c(\theta_c) = \frac{2V_p}{\lambda} \cdot \cos(\varphi_c) \cdot \frac{\sin(\theta_{crab} + \theta_c)}{\sin(\theta_c)} \cdot \theta_{3db\_0} \tag{29}$$

When $\theta_{crab} = 0$, we have

$$B_c(\theta_c) = \frac{2V_p}{\lambda} \cdot \cos(\varphi_c) \cdot \theta_{3db\_0} \tag{30}$$

From equation (30), it can be seen that the clutter spectrum is insensitive to azimuth scan angle in this special condition.

According to the parameters list in Tab.1, we obtain the following result.

According to Fig. 5, the following conclusion can be drawn.

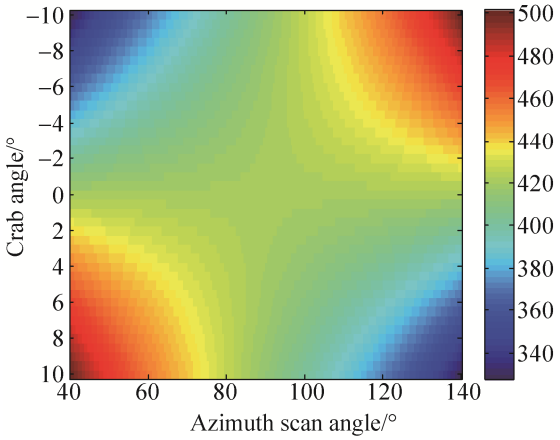


Fig. 5 Clutter spectrum distribution with the typical airborne system parameters (unit: Hz)

**Conclusion:** The fluctuation of clutter spectrum along the azimuth scan direction depends on the value of crab angle. When crab angle near or equal zero, the clutter spectrum will have little or no variation along the azimuth scan direction.

## 3.3 Multi-frequency system and multi-PRF system analysis

It is known that velocity ambiguities and blind velocities can be solved either by changing the radar wavelength between two bursts of pulses (multi-frequency system) or by changing the *PRF* (multi-PRF system) since they both depend on a

multiple integer of $\frac{\lambda \cdot PRF}{2}$. However, for range ambiguities, they depend on a multiple integer of $\frac{c}{2 \cdot PRF}$. This means that range ambiguities can only be solved by the multi-PRF system and it should be avoided in multi-frequency system design.

The range of *PRF* corresponding to the maximum unambiguous range $R_{max}$ can be calculated by

$$PRF \leqslant \frac{c}{2 \cdot R_{max}} \tag{31}$$

Then, we can obtain the following curve about *PRF* and $R_{max}$ in Fig.6.

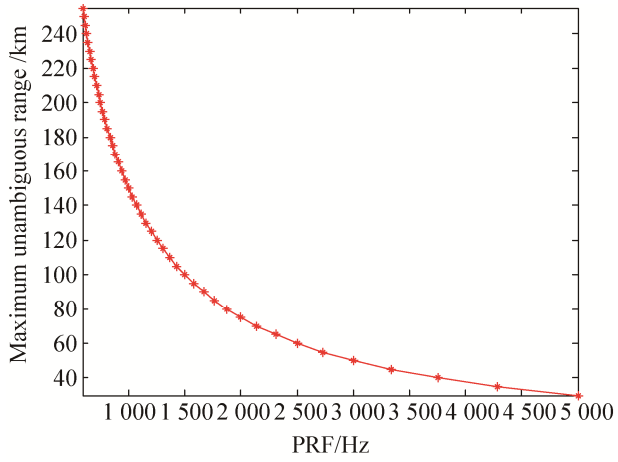


Fig. 6 Relation curve between system PRF and maximum unambiguous range

Therefore, to avoid range ambiguous in the multi-frequency system, the maximal value of PRF should decrease as the maximum operating range (system requirement) increases. This means that for the multi-frequency system with longer maximum operating range will have lower system PRF. It is known that WAS-GMTI system with high-PRF is more favorable for moving target detection than low-PRF system. Note that the PAMIR system is a multi-frequency system with a high PRF (6 000Hz), because its maximum operating range is short. Thus, we can make the following conclusion.

**Conclusion:** For WAS-GMTI system with relatively short maximum operating range, multi-PRF system and multi-frequency system are both selectable. However, for relatively long maximum operating range, multi-PRF system is preferred.

## 3.4 Number of pulses per burst analysis

For most WAS-GMTI systems, the same number of pulses is transmitted per burst in a scan operation. According to the basic knowledge of the antenna, transmit and receive antenna gain ($G_t(\theta_t,\varphi_t), G_r(\theta_t,\varphi_t)$) change with azimuth scan angles. These changes of antenna gain can lead to the different maximum operation ranges (since the SNR is affected) along the azimuth scan direction.

To compensate the aforementioned different antenna gain, we adjust the number of pulses per burst along the azimuth scan direction. The object is to make $G_t(\theta_t,\varphi_t)\times G_r(\theta_t,\varphi_t)\times\left(\sum_{i=1}^{K} w_i\right)^2 \Big/ \left(\sum_{i=1}^{K} w_i^2\right)$ approximately equal in every azimuth scan direction.

Taking the side-looking direction as the reference, the number of pulses per burst for difference scan directions can be designed based on the parameters list in Tab. 1. The calculated result is shown in Fig. 7(a).

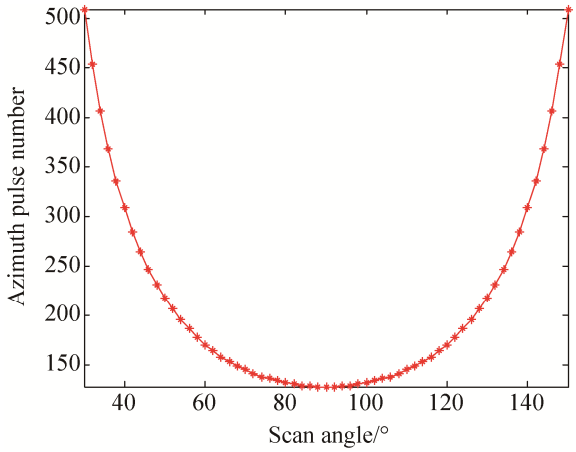


(a) Calculated number of pulsed per burst for different scan directions



https://dc-china-simulation.researchcommons.org/journal/vol30/iss12/34
DOI: 10.16182/j.issn1004731x.joss.201812034

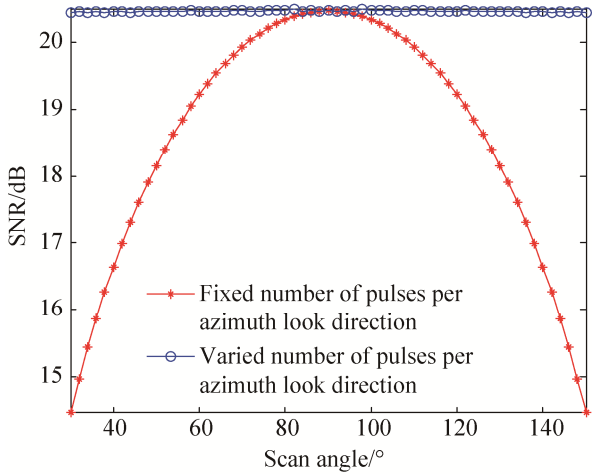


(b) SNR distribution with varied and fixed number of pulses per burst (70 dB chebyshev window, mean slant range 75 km)

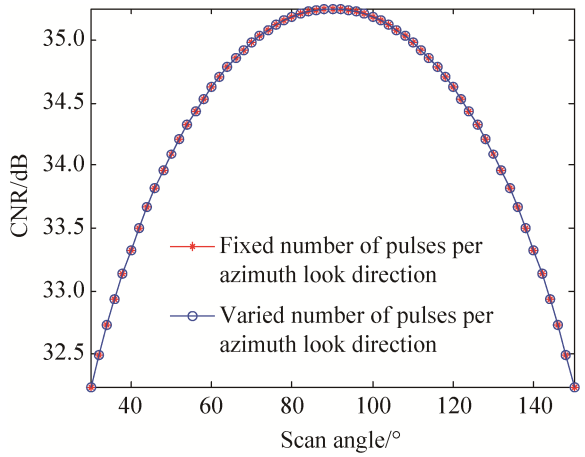


(c) CNR distribution with varied and fixed number of pulses per burst (70 dB chebyshev window，mean slant range 75 km)

Fig. 7 Number of pulses per burst analysis

It can be seen that more pulses are transmitted as the system scans away from the side-looking direction (scan angle is 90° for side-looking).

According to Equation (16), the SNR distribution of varied and fixed number of pulses per burst can be calculated in Fig. 7(b). Compared to the fixed number of pulses per burst, SNR keeps almost unchanged with the system that transmits different number of pulses along the azimuth direction. This is the main reason we design the varied number of pulses system.

Then, the CNR distribution is investigated in the same condition. As shown in Fig. 7(c), CNR is almost the same for the fixed and varied number of pulses system, and the reason can be found in Equation (16) and (19).

**Conclusion:** WAS-GMTI system with the varied number of pulses per burst can compensate the changes of transmit and receive antenna gain in the scan operation.

## 4 Discussions and Conclusions

This paper focuses on the problem of system design in WAS-GMTI radar system. Before our discussion, radar echo formula of WAS-GMTI mode and the expression of SNR and CNR are derived. These derivations are the foundations for the following research. Then, some key points are detailedly analyzed, including the expression for range walk and range curvature, the expression for clutter spectrum, selection of multi-frequency system and multi-PRF system, selection of number of pulses per burst. These four points and other considerations mentioned in the PAMIR system play an important role in our real WAS-GMTI system design. Besides, these key points should not be considered in isolation, they are mutual connection, mutual restraint. For example, the number of pluses per burst should be selected within some limits to reduce the influence of range walk. Therefore, we should carefully consider all these points and find a compromise between them.

## References:

[1] Cerutti-Maori D, Klare J, Brenner A R, et al. Wide-area traffic monitoring with the SAR/GMTI system PAMIR [J]. IEEE Transactions on Geoscience and Remote Sensing (S0196-2892), 2008, 46(10): 3019-3030.

[2] Cerutti-Maori D, Gierull C H, Ender J H G. Experimental verification of SAR-GMTI improvement experimental verification of SAR-GMTI improvement through antenna switching [J]. IEEE Transactions on Geoscience and

Remote Sensing (S0196-2892), 2010, 48(4): 2066-2075.
[3] Ender J H G, Berens P, Brenner A R, et al. Multi channel SAR/MTI system development at FGAN: From AER to PAMIR [C]// EUSAR, Köln, Germany, 2002. Germany: FGAN, 2002: 1697-1701.
[4] Cerutti-Maori D, Bürger W, Ender J H G, et al. Wide area surveillance of moving targets with the SAR/GMTI system PAMIR [C]// EUSAR, Dresden, Germany, May 2006. Germany: DLR, 2006.
[5] Ender J H G, Brenner A R. PAMIR-a wideband phased array SAR/MTI system [J]. IET Radar, Sonar & Navigation (S1751-8784), 2013, 150(3): 165-172.
[6] Yan H, Li F, Wang R, et al. Moving targets extraction in multichannel wide-area surveillance system by exploiting sparse phase matrix [J]. IET Radar, Sonar & Navigation (S1751-8784), 2013, 6(9): 913-920.
[7] Yan H, Zheng M J, Wang R, et al. Clutter suppression for multichannel wide-area surveillance systems via Kalman filtering [J]. IET Radar, Sonar & Navigation (S1751-8784), 2013, 7(3): 246-254.
[8] Guo B, Vu D, Xu L Z, et al. Ground moving target indication via multichannel airborne SAR [J]. IEEE Transactions on Geoscience and Remote sensing (S0196-2892), 2011, 49(10): 3753-3764.
[9] Wu D, Zhu D Y, Zhu Z D. Time-varying space-time autoregressive filtering algorithm for space-time adaptive processing [J]. IET Radar, Sonar & Navigation (S1751-8784), 2014, 6(4): 213-221.
[10] Zheng S, Song H, Wang R, et al. A space-borne wide-area surveillance mode and its application in maritime monitoring [J]. International Journal of Antennas and Propagation (S1687-5869), 2013: 1-9.
[11] Sun G C, Xing M D, Xia X G, et al. Robust ground moving-target imaging using deramp-keystone processing [J]. IEEE Transactions on Geoscience and Remote Sensing (S0196-2892), 2013, 51(2): 966-982.
[12] Eduaro M, Antoni B, Josep R, et al. A Performance Evaluation of SAR-GMTI Missions for Maritime Applications [J]. IEEE Transactions on Geoscience and Remote Sensing (S0196-2892), 2015, 53(5): 2496-2509.
[13] Liu B C, Yin K Y, Li Y K, et al. An Improvement in Multichannel SAR-GMTI Detection in Heterogeneous Environments [J]. IEEE Transactions on Geoscience and Remote Sensing (S0196-2892), 2015, 53(2): 810-827.
[14] Eduaro M, Stefan V B, Marc J, et al. Multichannel SAR-GMTI in Maritime Scenarios with F-SAR and TerraSAR-X Sensors [J]. IEEE Journal of Selected Topics in Applied Earth Observations and Remote Sensing (S1939-1404), 2015, 8(11): 5052-5067.
[15] Yan H, Zhu D Y, Wang R, et al. Practical Signal Processing Algorithm for Wide-area Surveillance-GMTI Mode [J]. IET Radar, Sonar & Navigation (S1751-8784), 2016, 9(8): 991-998.

## 《系统仿真学报》荣获“2017 中国国际影响力优秀学术期刊”证书

由中国学术期刊（光盘版）电子杂志社与清华大学图书馆联合成立的中国学术文献国际评价研究中心，发布了 2017 版《中国学术期刊国际引证年报》，《系统仿真学报》荣获“2017 中国国际影响力优秀学术期刊”。

《年报》（2017 版）采用的统计源期刊为 20192 种，涵盖 WoS 收录的 SCI 期刊 8874 种、SSCI 和 A&HCI 期刊 4645 种，ESCI 期刊 5578 种；增补期刊 1762 种。参照中外文学术期刊总被引频次、影响因子、半衰期等各项国际引证指标，计算期刊影响力指数(CI)，对国内 6210 种学术期刊排序，遴选了人文社科、自然科学与工程技术两个类别的 TOP10%为国际影响力品牌学术期刊。TOP5%以内的期刊为“最具国际影响力学术期刊”、TOP5-10%之间的为“国际影响力优秀学术期刊”。




DOI: 10.16182/j.issn1004731x.joss.201812034